Eur. Phys. J. B **9**, 605–611 (1999)

THE EUROPEAN PHYSICAL JOURNAL B

EDP Sciences

Collapse of the magnetic ordering and structural anomalies in the $U_xLa_{1-x}S$ system: neutron diffraction and specific heat measurements

F. Bourdarot[1], A. Bombardi[1,2,a], P. Burlet[1], R. Calemczuk[1], G.H. Lander[2], F. Lapierre[1], J.P. Sanchez[1], K. Mattenberger[3], and O. Vogt[3]

[1] Département de Recherche Fondamentale sur la Matière Condensée, SPSMS, CEA/Grenoble, 38054 Grenoble Cedex 9, France
[2] European Commission, JRC, Institute for Transuranium Elements, Postfach 2340, 76125 Karlsruhe, Germany
[3] Laboratorium für Festkörperphysik, ETH-Zürich, 8093 Zürich, Switzerland

Received 18 September 1998

Abstract. We report specific heat and neutron diffraction measurements of seven samples in the solid solution system $U_xLa_{1-x}S$. All samples have the simple fcc NaCl crystal structure. Both specific heat and neutron diffraction confirm the suggestion from the earlier magnetic measurements that the ferromagnetism disappears abruptly at $x_c \sim 0.57$. Near x_c there is a doubling of γ the electronic contribution to the specific heat, as compared to the value of 23 mJ $mol^{-1}K^{-2}$ in pure US. Around x_c the widths of the nuclear Bragg peaks show a considerable broadening, as well as anomalies in the mean lattice parameter, as compared to those expected from Vegard's law. A preliminary analysis suggests this broadening may be due to a loss of long range lattice order near x_c. However, these changes are independent of temperature, so that further experiments are necessary before they can be associated with the changes in magnetic behavior at x_c.

PACS. 75.25+z Spin arrangements in magnetically ordered materials (including neutron and spin-polarized electron studies, synchrotron-source x-ray scattering, etc.) – 61.66.-f Structure of specific crystalline solids – 65.40.+g Heat capacities of solids

1 Introduction

The monopnictides and monochalcogenides of uranium, neptunium and plutonium [1] with the simple NaCl type structure exhibit a wide variety of magnetic and electronic behaviors which are generally considered as a consequence of variable degree of localization of the $5f$ electrons. In general the interactinide distances are large enough to prevent direct overlap of the $5f$ electrons but hybridization effects occur via the anions p orbitals or are mediated by valence and conduction band electrons [2]. Among these compounds the uranium monochalcogenides (US, USe, UTe) are classified as strongly hybridized [1]. As shown in Table 1 they order ferromagnetically at rather high temperature and are highly anisotropic ferromagnets with magnetic moments confined along the $\langle 111 \rangle$ directions. The ordered magnetic moment at low temperature as well as paramagnetic moments are much lower than the values expected for trivalent or tetravalent uranium free ions.

In spite of many theoretical and experimental efforts devoted to the electronic and magnetic properties of these compounds, a clear understanding of their electronic structures and of the mechanisms responsible of their behavior is still lacking. In particular, the ground state and the respective influence of crystal field and interactions, which involve hybridization effects, are not easy to determine. For these ferromagnetic compounds the dilution of the paramagnetic ions by diamagnetic ones reduces the exchange, thus giving access to the single-ion characteristics. However the studies of such diluted uranium systems have revealed complex behavior different from that expected for a simple dilution of the magnetic interactions, *i.e.* a linear decrease of the ordering temperature and a constant value of the ordered moment for a concentration of paramagnetic ions larger than the critical percolation limit for this fcc structure.

In uranium sulfide diluted either by trivalent (La) or tetravalent (Th) diamagnetic ions an abrupt disappearance of the ferromagnetic order occurs at an uranium concentration far above the percolation limit ($x \sim 0.14$) for the fcc lattice. In the US-ThS system Danan *et al.* [3] gave a critical concentration $x_c(U)$ between 0.4 and 0.6 for the disappearance of the ferromagnetic ordering. From specific heat measurements they showed an increase of the low-temperature electronic term γ for Th concentrations close to this critical concentration. They interpreted the disappearance of the long range ordering by a crystal-field

[a] e-mail: bombardi@drfmc.ceng.cea.fr

Table 1. Some physical properties of the uranium monochalcogenides after [1]. The evolution of the magnetic quantities as the lattice parameter increases suggests a progressive localization of f electrons. (* Intermediate coupling).

		a(Å)	T_C(K)	paramagnetic moment (μ_B/U)	ordered moment (μ_B/U)
US		5.489	180	2.35	1.70
USe		5.744	160	2.40	2.00
UTe		6.155	104	2.60	2.25
U	U^{4+}			3.67 $(5f^2)$*	3.28 $(5f^2)$*
free ions	U^{3+}			3.78 $(5f^3)$*	3.42 $(5f^3)$*

effect assuming a divalent state for the U ions. Such a divalent state for an early actinide ion is now regarded as improbable. In addition, since we believe US has an electronic structure close to U^{3+}, doping with Th^{4+} changes the character of the conduction band.

More recently, Schoenes *et al.* [4] in their study of single crystals in the US-LaS solid solutions find a critical concentration of U close to $x = 0.6$. The magnetization measured at low temperature in a field of 9.5 T along the three principal directions gives a constant magnetic moment of about 1.55 μ_B/U for uranium concentrations larger than 0.6 and indicates a strong anisotropy along the $\langle 111 \rangle$ easy axes. Around $x = 0.6$ the magnetic moment drops to 0.3 μ_B/U (in 9.5 T) and the magnetization becomes isotropic (*i.e.* similar values for three symmetry directions are found). In the paramagnetic range the analysis of the magnetic susceptibility leads to a nearly constant value of the effective moment and to a nearly linear decrease of the Curie-Weiss temperature, whereas the constant Pauli susceptibility term χ_0 increases strongly on crossing the critical concentration. From a careful analysis of susceptibility, magnetization, and transport data, the authors concluded that the degree of localization in these compounds varies nonmonotonically and that hybridization and magnetic exchange play dominant roles.

In the present paper we report results of specific heat and neutron diffraction measurements on single crystals with different uranium concentrations within the US-LaS system, similar to those of Schoenes *et al.* [4]. The specific heat measurements establish the ordering transition temperature and the low-temperature electronic contribution. The neutron scattering gives a microscopic description of the magnetic ordering, and also shows structural anomalies around the critical concentration (lattice parameter, degree of order of the solid solution). After a description of the experimental conditions we will focus on the evolution of the magnetic ordering in these compounds.

2 Experimental

The single crystals have been grown at ETH Zürich by the mineralisation technique [5]. They have parallelepiped shape with faces perpendicular to the cubic axis, and dimensions of a few mm along each axis.

The neutron diffraction experiments have been performed with the D15 diffractometer, which is installed at the high flux reactor of ILL. The wavelength was 1.172 Å. Samples with uranium concentration $x = 0.30$, 0.40, 0.50, 0.55, 0.60, 0.80 and 0.90 have been studied. The lattice parameters have been determined at room temperature and low temperature from the positions of a large number of nuclear reflections. Integrated intensities have been measured to check the nuclear and magnetic structures. For the low temperature studies a conventional cryostat was used. The Curie temperature and the magnetic moment variations were determined by measuring the intensities of several Bragg peaks as a function of temperature. Some samples have also been checked by X-ray diffraction at room temperature to verify the lattice parameters anomalies found in neutron experiments. The apparatus used to measure the heat capacity is an improved version of the adiabatic, continuous heating technique. The heat capacity is given by $C = P/(\mathrm{d}T/\mathrm{d}t)$. The approximately constant power P is set to obtain a predetermined average heating rate [6].

3 Magnetic ordering

Ferromagnetic order has been found in all samples with $x \geq 0.6$. This is shown in Figure 1 for $x = 0.80$ and $x = 0.60$ by extra intensity developing at the same position as the nuclear peaks. As shown in Figure 2a, the Curie temperature decreases linearly with x for $0.6 \leq x \leq 1$ and extrapolates to $T_C = 0$ K at $x = 0$. The ordered uranium magnetic moment at low temperature (5 K) (Fig. 2b) is nearly independent of x for $0.60 < x \leq 1$, but at $x = 0.60$ a significantly lower value of 0.8(2) μ_B/U is found. For $x > 0.6$ the moment is similar to that measured by neutron diffraction in pure US, $m = 1.70(2)$ μ_B/U [7], and higher than the value deduced from magnetization measurements [8]. This difference between neutron and magnetization values is normally ascribed to the conduction electron polarisation. Samples with $x \leq 0.55$ do not show any additional ferromagnetic scattering down to the lowest temperatures (5 K). Allowing for statistics we may place an upper limit of 0.2 μ_B/U for such a component. As the disappearance of the ferromagnetic component could be due to the transition to an antiferromagnetic state, a search for an antiferromagnetic contribution was

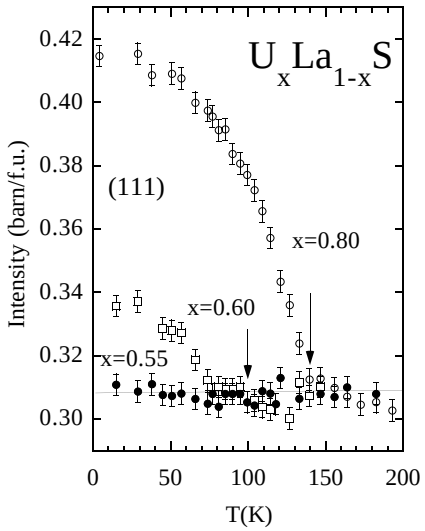

Fig. 1. Change of intensity observed at the (111) reflection as a function of temperature for three values of x. The increase in intensity corresponds to a ferromagnetic component for $x = 0.60$ and $x = 0.80$. The arrows mark T_C.

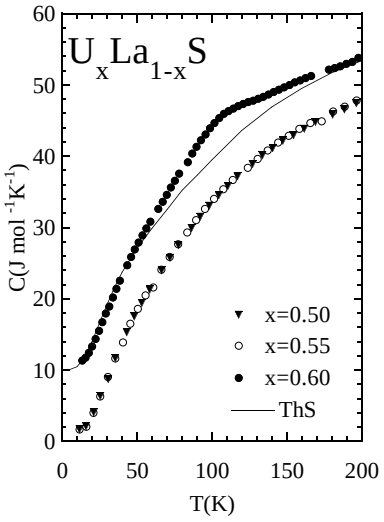

Fig. 3. Specific heat for $x = 0.50$, 0.55 and 0.60. The curve corresponding to ThS [3] is also shown. The values for $x = 0.60$ and ThS are shifted by 10 J mol^{-1}K^{-1}. For $x = 0.60$ an extra contribution is clearly observed.

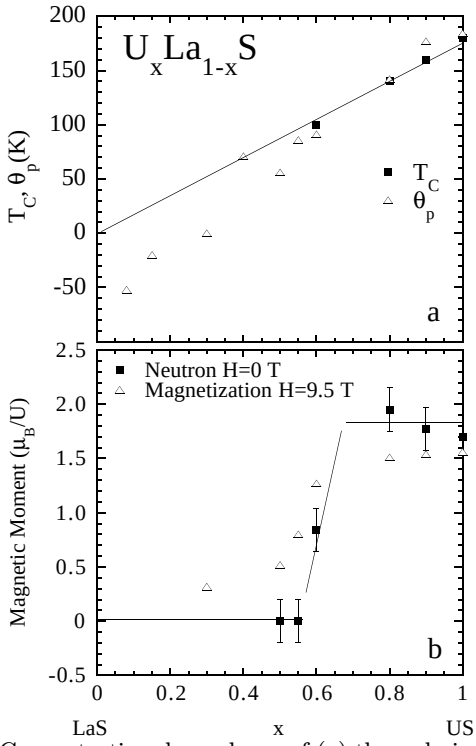

Fig. 2. Concentration dependence of (a) the ordering temperature (T_C) and the paramagnetic Curie temperature (θ_p) and (b) of the uranium ordered magnetic moment at $T = 5$ K.

undertaken, but no new satellites were found, or any sign of diffuse scattering. This is consistent with the absence of any sign of any antiferromagnetic transition in the susceptibility measurements.

The results of specific heat measurements shown in Figure 3 for samples with $x = 0.60$ (still ferromagnetic with $T_C = 100$ K) $x = 0.55$ and 0.50 (not ferromagnetic) ascertain that the disappearance of the ferromagnetic contribution corresponds to the loss of any cooperative magnetic order. The curves for $x = 0.50$ and $x = 0.55$, very similar to that of ThS [3], represent only the lattice and electronic contributions whereas for $x = 0.6$ an extra contribution is clearly observed. This develops below 200 K down to 50 K with a maximum around $T = 100$ K, a temperature corresponding to the ordering temperature ($T_C = 100$ K) determined by neutron diffraction. These results confirm the abrupt disappearance of long-range ordering in compositions between $x = 0.55$ and $x = 0.60$.

The samples with $x > 0.60$ order ferromagnetically with a $\langle 111 \rangle$ easy axis. This results in a large rhombohedral distortion [9]. This is best observed by measuring reflections of the form {hhh}; however, because all 4 possible $\langle 111 \rangle$ axes can be the moment direction in a zero-field cooled single crystal, the rhombohedral distortion results in a broadening of the mosaic of *all* reflections. Thus, although the exact magnitude of the distortion cannot be measured at the (006), which would normally not split with such a distortion, its presence is easy to detect. This is shown in Figure 4 for the $x = 0.80$ sample. At the same time we show the much wider, but temperature independent FWHM, observed in the $x = 0.55$ and 0.60 samples.

From these experiments one can conclude that, within the experimental accuracy, the ferromagnetic ordering vanishes abruptly at the critical concentration $x_c = 0.57 \pm 0.02$, below which no long-range ordering exists. This magnetic-non magnetic transition may be connected with changes in the electronic structure, which could be reflected by the electronic coefficient γ. The plots of C/T *versus* T^2 of the low-temperature specific heat are given in Figure 5. They lead to relatively low electronic values $\gamma \approx 40$ mJ mol^{-1} K^{-2} (see Tab. 2) increasing near

Table 2. The results obtained at different x for various physical quantities are shown. The values of the lattice parameters a, as measured by neutron scattering (NS) at room and low temperature (RT, LT) and by X-rays are consistent and give the same anomalous behaviour around x_c. The FWHM is of the (006) nuclear reflection at room temperature. The evolution of T_C and m, obtained using the form factor given in [7] compared with the values of the moment induced at low temperature with H = 9 T are shown. γ is the coefficient of T^2 in the low-temperature specific heat; the values for US is taken from Westrum [14].

x		a(Å)		(006)	T_C	$m(\mu_B)$	$m(\mu_B)$	γ
	RT	RT	LT	FWHM	(K)	NS	Ref. [4]	(mJ mol^{-1}K^{-2})
	NS	X-rays	NS	(deg.)		H = 0 T	H = 9.5 T	(±1)
	(±0.005)	(±0.001)	(±0.005)	(±0.01)		(±0.2)		
0		5.860						
0.30	5.753			0.31			0.3	
0.40	5.719	5.703		0.31				
0.50		5.740	5.705	0.68		0.0	0.5	44
0.55	5.719	5.716	5.697	0.65		0.0	0.78	45
0.60	5.630	5.622	5.622	0.59	100	0.8	1.25	30
0.80		5.541	5.548	0.36	140	1.9	1.51	
0.90	5.514		5.508	0.31	160	1.8	1.53	
1		5.489			180	1.70(2)	1.55	23

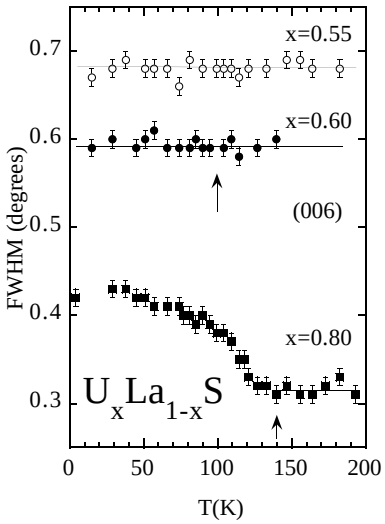

Fig. 4. FWHM for the (006) nuclear reflection as a function of temperature for x = 0.55 (non ordered), x = 0.60 (T_C = 100 K) and x = 0.80 (T_C = 140 K). The arrows mark T_C.

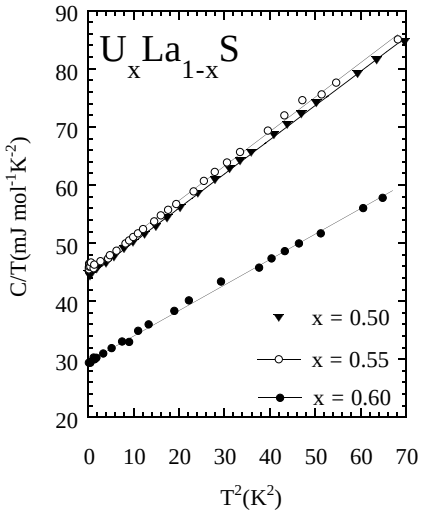

Fig. 5. C/T *vs.* T^2 for x around the critical concentration.

the critical concentration, a behavior similar to that observed in the solid solutions $U_xTh_{1-x}S$ [3]. This is to be compared with a value of γ = 23 mJ mol^{-1}K^{-2} for pure US.

4 Structural characterization

The concentration dependence of the measured cell parameter $a(x)$ determined by neutron and X-ray diffraction is shown in Figure 6. The experimental values follow a Vegard law, however, a marked anomaly is seen around x = 0.50, where the measured values are significantly higher than those expected for a linear relationship. The deviation of about 0.05 Å is much larger than the experimental accuracy (0.005 Å), and cannot be attributed to deviation of the solid solution from its nominal concentration x because the deviation would then be $\sim 10\%$ which is incompatible with the synthesis and crystal growth techniques.

Refinement of the nuclear reflections assuming stoichiometry and the nominal cation concentration x gives good agreement between observed and calculated structure factors (residual factor $R = \frac{\sum |F_{obs} - F_{cal}|}{\sum F_{obs}} \approx 0.02$) without including any extinction correction. The limited number of independent reflections measured in these experiments (a consequence of the high fcc symmetry) does

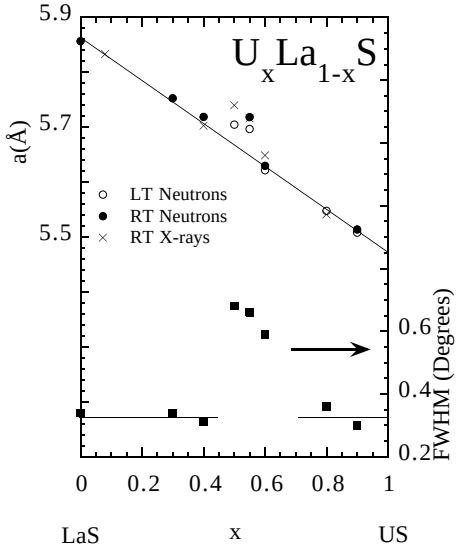

Fig. 6. Cell parameter a and FWHM at low temperature (LT) of the (006) nuclear reflection as a function of the uranium concentration. The cell parameter follows a Vegard law except around $x \sim 0.55$ where it is significantly higher than expected, in the same range of concentrations the width of the reflection is larger than the instrumental resolution.

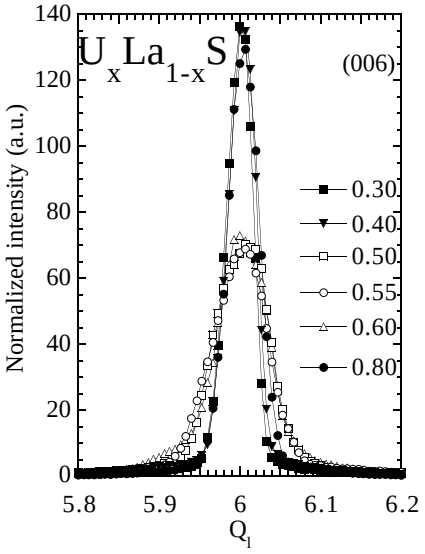

Fig. 7. Profile of the (006) reflection for various x values. Around $x \sim 0.55$ (open symbols) the FWHM is larger than the instrumental resolution. The areas are normalised to the same value for all the concentrations.

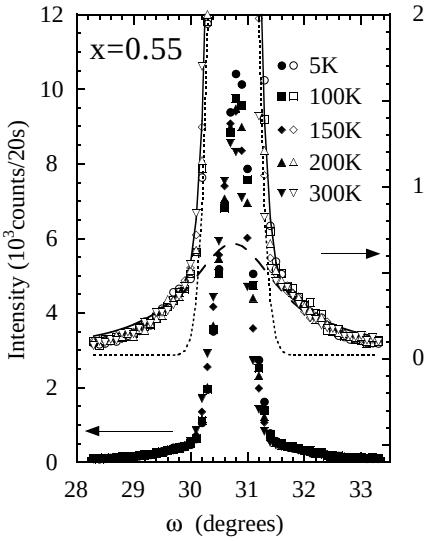

Fig. 8. Temperature dependence of the (006) reflection for $x = 0.55$ taken with an omega (ω) scan with only the crystal moving. Curves are plotted on different scales to emphasize the Bragg peak (dots) and the weak diffuse contribution (dashes).

not allow a reliable estimate of the individual Debye-Waller factors for the two atomic species, and nominal values have been used.

The shape of the Bragg peaks (measured at room temperature) shows an anomaly in the range of composition where the lattice parameter deviates from the Vegard law. As illustrated in Figure 7, which displays longitudinal scans around the (006) Bragg reflection, narrow peaks with FWHM corresponding to the instrumental resolution are observed for all concentrations outside the critical range. In contrast, for compositions around the critical concentration ($x = 0.50$, 0.55, 0.60) a much larger width, twice that of the instrumental resolution is found. For any concentration the profile cannot be reproduced by a single contribution of either Gaussian or Lorentzian type. Fits including both contributions give an agreement factor χ^2 one order of magnitude smaller than single peak fitting. The Gaussian contribution is by far the strongest and essentially determines the FWHM, but the Lorentzian is necessary to model the intensity in the wings of the peak, see Figure 8. The profile of the reflection is temperature independent with simply a small reduction in intensity of the Gaussian contribution as the temperature increases due to the Debye-Waller factor. The absence of any temperature dependence of the diffuse intensity implies that it cannot arise from thermal diffuse scattering, and must be due to structural inhomogeneities. Its FWHM has a broad maximum around $x \sim 0.50$. This diffuse scattering also has a strong Q dependence as is seen in Figure 9.

Focusing now on the Gaussian FWHM, we plot its FWHM in Figure 10 for two different compositions at room temperature. The value for $x = 0.30$ corresponds to the instrumental resolution curve which assumes a large coherence length and a small mosaic spread of the crystal to give resolution limited Bragg peaks. In contrast, in the critical range ($x = 0.55$) the FWHM departs strongly from this curve. However at low angle the two curves extrapolate to the same value which means that the broadening is Q dependent.

The broadening of the Bragg peaks, see Figure 10, as a function of scattering angle follows closely the particle size broadening formula (Scherrer equation) with a $(\cos\theta)^{-1}$ dependence [10]. Using the standard formula in which the inverse particle size and resolution functions add approximately in quadrature, we can deduce a particle size ξ as

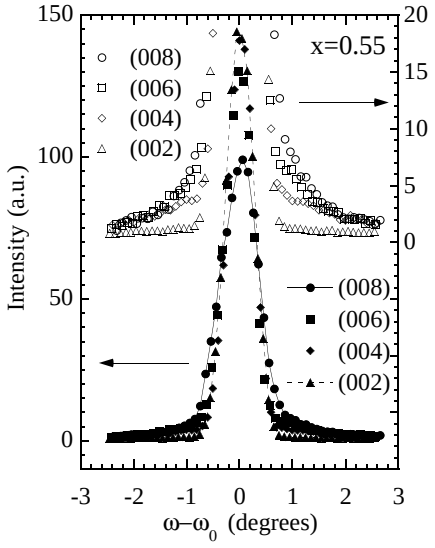

Fig. 9. ω-scan profiles of the (00l) (l = 2, 4, 6, 8) reflection for $x = 0.55$. ω_0 are the centers of the reflections.

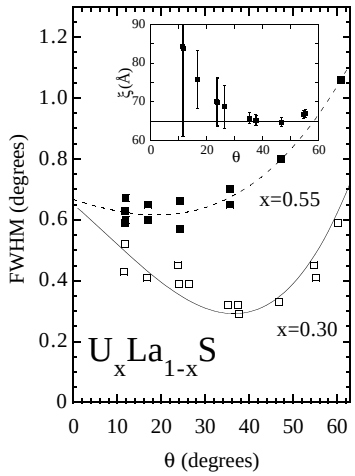

Fig. 10. FWHM of ω-scans *vs.* the scattering angle for $x = 0.30$ and $x = 0.55$. The solid line is the resolution curve of the spectrometer, the dashed one is a polynomial fit of the data. The inset shows the particle sizes derived from the Scherrer equation (see text) after deconvoluting with the instrumental resolution.

a function of scattering angle. This is shown as the inset in Figure 10. The fact that ξ is constant confirms this as a possible explanation for the broadening of the Gaussian part of the profile. However such a small value of $\xi \approx$ 65 Å is certainly unusual in such a highly symmetric material. One would expect particle sizes to exceed at least 500 Å, based on experiments on other NaCl-type uranium compounds. The Lorentzian-like wings of the scattering no doubt also come from local homogeneities. Note that since the coherent amplitudes of U (0.854) and La (0.824) are very similar it cannot arise from correlations between these two species, which are indistinguishable by neutron scattering. Some positional short-range order (perhaps coupled to cation ordering) may be at the origin of this scattering.

5 Discussion

From the result of the present study and those of Schoenes *et al.* [4] it is clear that in the $U_xLa_{1-x}S$ solid solutions long range magnetic ordering abruptly disappears at a critical concentration $x_c = 0.57(2)$. This concentration is far above the percolation limit, below which only finite clusters of connected paramagnetic ions exist. It has been experimentally observed for isostructural compounds like the monoxides NiO and CoO [11] that the long range (antiferromagnetic) order persists to the concentration of paramagnetic ions corresponding to the bond percolation limit in the fcc lattice. This situation was observed experimentally in the isostructural ferromagnetic EuS compound diluted by non magnetic SrS. For Eu concentration below the percolation limit (0.14), the system behaves like a superparamagnet with spin dynamics that follow a model with random Eu clusters with intra and intercluster dipolar energies [12]. In our case the critical concentration is so high that any percolation argument can be excluded to explain the absence of ordering below x_c.

For uranium concentration higher than $x = 0.60$ a similar behavior as in pure US is observed. The ordered low temperature moment and the magnetic anisotropy are not affected by dilution. The scaling of T_C and θ_p with the uranium concentration indicates a simple dilution of the exchange interactions. The susceptibility parameters (χ_0, μ_{eff}) keep the same value as in US and the electrical resistivity is typical of ferromagnetic compounds.

Around the critical composition we have observed a number of unusual effects. The first (see Tab. 2) is that the electronic coefficient to the specific heat (γ) approximately doubles in this range. Although γ is small by standards of heavy-fermion materials, the doubling near the critical composition suggests a change in the electronic structure. The second unusual effect is the observation of *structural anomalies*, even at room temperature. The lattice parameters are significantly larger than predicted by Vegard's law near $x \sim 0.50$, although they follow such a law on both sides of this composition. The widths of the Bragg peaks are considerably larger (a factor of two depending on the Q value – see Fig. 10). We have analysed these data with the Scherrer equation to give a particle size of approximately 70 Å, which is far smaller, by at least an order of magnitude, than normally found for this type of solid solution. Further experiments are planned to investigate this aspect of the crystals. The effect itself is unrelated to magnetism as it is independent of temperature, but the interesting question is whether it is related to the change in the electronic structure at this composition, for example, as a consequence of an increased ionic size for the uranium and a subsequent loss of miscibility

in the solid solution. Further experiments are needed to address this point.

The sudden loss of magnetism at a fairly high U concentration, which our experiments have confirmed in the (U,La)S solid solutions, are consistent with earlier work by Danan *et al.* [3] on the (U,Th)S system, where $0.4 < x_c < 0.6$. They did not report any structural anomalies, but the effects reported in the present paper would be difficult to observe in polycrystalline samples as used by Danan *et al.* Recently, Cooper and Lin [13] have developed an *ab initio* approach to address the moment collapse in the diluted U chalcogenides and we hope that this work, and future planned experiments, will act as a stimulus for this and other theories.

The authors thank J. Pécout for his help with X-rays measurements and B.R. Cooper for discussions. Support to A.B. from the TMR programme (contract 98/04 cat.20) of the European commission is acknowledged.

References

1. O. Vogt, K. Mattenberger, *Handbook on the Physics and Chemistry of the Rare Earths*, edited by K.A. Gschneidner Jr., L. Eyring, G.H. Lander, G.R. Choppin (North Holland, 1993), Vol. 17.
2. B.R. Cooper, in *Handbook on the Physics and Chemistry of the Actinides*, edited by A.J. Freeman, G.H. Lander (North Holland, 1984), Vol. 1.
3. J. Danan, C.H. de Novion, Y. Guerin, F.A. Wedgwood, M. Kuznietz, J. Phys. France **37**, 1169 (1976); M. Haessler, C.H. de Novion, J. Phys. C **10**, 589 (1977).
4. J. Schoenes, O. Vogt, J. Loehle, F. Hulliger, K. Mattenberger, Phys. Rev. B **53**, 14987 (1996).
5. O. Vogt, in *Actinides in Perspectives*, edited by N.M. Edelstein (Pergamon, Oxford, 1982); J.C. Spirlet, O. Vogt, *Handbook on the Physics and Chemistry of the Actinides*, edited by A.J. Freeman, G.H. Lander (North Holland, 1984), Vol. 1.
6. A. Junod, E. Bonjour, R. Calemczuk, J.Y. Henry, J. Muller, G. Triscone, Physica C **211**, 304 (1993).
7. F.A. Wedgwood, J. Phys. C **5**, 2427 (1972); G.H. Lander, M.S.S. Brooks, B. Lebech, P.J. Brown, O. Vogt, K. Mattenberger, J. Appl. Phys. **69**, 4803 (1991).
8. D.L. Tillwick, P. De V. Duplessis, J. Magn. Magn. Mater. **3**, 329 (1976).
9. G.H. Lander, M.H. Mueller, Phys. Rev. B **10**, 1994 (1974).
10. B.E. Warren, X-ray diffraction (Addison Wesley, 1969), p. 253.
11. A.Z. Menshikov, Yu.A. Dorofeev, N.A. Nironova, M.V. Medvedev, Solid State Commun. **98**, 839 (1996).
12. G. Eiselt, J. Koetzler, H. Maletta, D. Stauffer, K. Binder, Phys. Rev. B **19**, 2664 (1979).
13. B.R. Cooper, Y.L. Lin, J. Appl. Phys. **83**, 6432 (1998).
14. E.F. Westrum, R.R. Walters, H.E. Flotow, D.W. Osborne, J. Chem. Phys. **48**, 155-161 (1968).